An experimental and analytical investigation on the hydrodynamic efficiency of a cylindrical oscillating water column wave energy device

Saishuai Dai*[1], Sandy Day[1] and Qing Xiao[1]

Naval Architecture, Ocean and Marine Engineering, University of Strathclyde, G1 0LZ, United Kingdom

Abstract: Three-dimensional cylindrical Oscillating Water Column (OWC) wave energy device is investigated in this work using both experimental and analytical methods. Non-linear Power take off system is simulated by an orifices-plate. Three different damping levels' effects are studied. Results show that analytical method combining damping effect, taken from experiment, can provide a better prediction for the experiment. However, analytical method fails to include viscous effect. In addition, present results also suggests that in low wave frequency region, high damping leads to a better performance in capture factor as compared to a low damping case.

Keywords: wave energy device; oscillating water column; experimental study; analytical study;
Article ID:

1. Introduction

OWC wave energy converters (WECs) have being one of the most popular WECs since it appeared as a navigation buoy proposed by Yoshio Masuda in 1965 (Falcão 2010). An OWC WEC usually comprises two main parts: an air chamber partially immersed in water with open at the bottom and a power take off (PTO) system, which is usually a self-rectified turbine. When encountered with incident waves, water column's motion inside the chamber forces trapped air to flow through the turbine, electricity is then generated by utilizing the rotation of turbine. Detailed information of OWC devices' technology can be found in several reviews, for instance, Thorpe (1999) ~~ect~~.

The simple working principle of this type WECs and its huge potential of capturing wave energy attracted many researchers' efforts in both analytical and experimental. For analytical works, Evans (1978) deduced the maximum efficiency for a symmetrical OWC device by considering the internal surface as a rigid weightless piston. Therefore, the spatial variation of the internal water surface was ignored. As an extension of Newman's (1974) work, the width of the internal free surface was assumed to be small comparing with the incident wavelength. Based on the study of Stoker (1957), Falcão and Sarmento (1980) considered the spatial variation of the internal free surface by introducing a periodic pressure distribution. Their work was generalised to arbitrary pressure distributions in both two and three dimensions by Evans (1982). Later on, Evans and Porter (1995) published an efficient, accurate method to compute the hydrodynamic coefficients and optimized maximum theoretical efficiency of a two dimensional harbour like OWC device based on pressure distribution model. More recently, Martins-Rivas and Mei, (2009) studied an OWC device installed at the tip of a breakwater. Şentürk and Özdamar (2012) studied an OWC WEC with a gap on the fully submerged front wall. On the other hand, earlier reported work on experiment study of two-dimensional OWC WECs can be traced back to 1980s. For example, Maeda, e~~ct~~ ~~-~~al. (1985) carried out a fixed OWC experiment to validate their equivalent floating body theory. Sarmento (1992) measured the hydrodynamic efficiency of symmetrical and asymmetrical OWC devices and validated their pressure distribution model. It is worthy to mention that in his study, efficiency was calculated based on reflection and transmission coefficients. Therefore, damping effect of the PTO system was not taken into account. This resulted in the efficiency of experiment being slightly larger than that of theoretical maximum efficiency. With an experiment, Whittaker and Stewart (1993) found that if the damping is properly selected, OWC with a harbour can achieve a widen bandwidth of power extraction. Later on, Wang et al. (2002) investigated the effect of bottom slop topography and water depth on the performance of an OWC. Morris-Thomas, Irvin and Thiagarajan (2007) examined the effect of front submerged wall and validated their result against Evans and Porter's theoretical result.

All of the above mentioned works are focused on rectangular shaped near-shore or shoreline OWC WECs and few papers are found for cylindrical OWC devices. Probably, this is leaded by the result from Evans and Poter (1997), where they concluded that the optimal capture width

Received date:
***Corresponding author Email: Saishuai.dai@strath.ac.uk**

for an axisymmetric cylindrical OWC device is generally very low, and thus is less attractive for long-term exploration. However, compared with rectangular type OWC devices, the performance of cylindrical OWC devices is independent of the incident wave direction. This makes them much suitable in offshore application, where incident wave direction is rather random while wave energy intensity is much higher than near-shore and shoreline. Therefore, the study on cylindrical OWC is still valuable. In this paper, an investigation of axisymmetric cylindrical OWC WEC with PTO system modelled by an orifices-plate is carried out to examine its hydrodynamic performance. Results are validated against Evans' pressure distribution theory. In the following sections, theory of pressure distribution will be firstly introduced briefly. Section 3 will discuss experiment facilities and procedures. Results will be presented and discussed in section 4. Section 5 will give discussion and conclusions.

2. Theory of Evans and Porter

The basic principal of pressure distribution model is assuming that there exists an oscillating pressure with the same frequency as incident wave upon the free surface inside the OWC device. By relating the relative pressure with the air volume flux inside the chamber induced by incident wave with a turbine characteristic, the problem is simplified to a hydrodynamic problem via solving velocity potential.

Since Evans & Porter's (1997) model is extensively used, an extension on how to calculate the mean power absorbed is made in the present work. Therefore, we only describe the ~~ensential~~ essential proceducers on deriving the hydrodynamic efficiency (capture factor) and subsequent changes are addressed. Details on solving the numerical problem should refer to Evans & Poter (1997) and Evans (1982).

Assuming the cylindrical device with radius b is coordinated as shown in Fig 1~~Fig 1~~, enclosing an internal free surface S_I and draft equals to a. External free surface is denoted by S_E and h is the constant water depth. According to pressure distribution model, we define the pressure distibution as $p_a + p(\mathrm{x},t)$, where p_a is the atmospheric pressure and $p(\mathrm{x},t)$ is the oscillating pressure (dynamic pressure) with same frequency ω as the incident wave. Assuming that the horizontal oscillating pressure variation across S_I is negligable, then oscillating pressure becomes only time dependent variable $p(t)$.

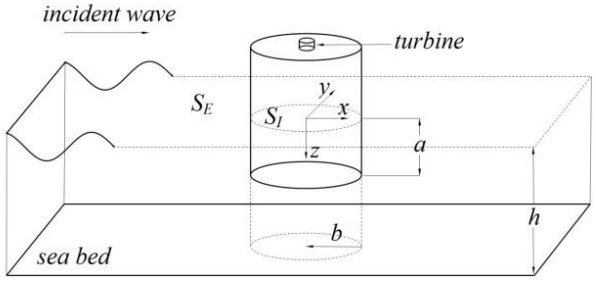

Fig 1 Sketch of the analytical problem

According to linear wave theory (for instance, Mei (2005)) , the velocity potential $\phi(x,y,z,t)$ satisfies the following equations as

$$\nabla^2\phi = 0, \quad \text{in the whole fluid domain} \tag{1}$$

$$\phi_n = 0, \quad \text{at seabed and OWC device body surface} \tag{2}$$

Where n is the normal derivative of seabed and OWC device structure. On the free surface the following conditions hold

$$g\eta - \frac{\partial\phi}{\partial t} = \begin{cases} \dfrac{p_a + p(t)}{\rho}, & \text{on } S_I \\ \dfrac{p_a}{\rho}, & \text{on } S_E \end{cases} \tag{3}$$

$$\frac{\partial\eta}{\partial t} = \frac{\partial\phi}{\partial z}, \quad \text{on z=0} \tag{4}$$

Where $\eta(x,\mathrm{y},\mathrm{t})$ is the surface elevation, ρ is the density of fluid, g is gravitational acceleration

It is assumed that the motion is time-harmonic and thus it is not difficult to introduce time-independent quantities by

$$\phi(x,y,z,t) = \mathrm{Re}\{\hat{\phi}(x,y,z)e^{-i\omega t}\} \tag{5}$$

$$p(\mathrm{t}) = \mathrm{Re}\{\hat{\mathrm{p}}e^{-i\omega t}\} \tag{6}$$

$$\eta(x,y,t) = \mathrm{Re}\{\hat{\eta}(x,y)e^{-i\omega t}\} \tag{7}$$

$$Q(t) = \mathrm{Re}\{\hat{q}e^{-i\omega t}\} \tag{8}$$

Where $\hat{\phi}$, $\hat{p}$ and $\hat{\eta}$ is the complex amplitude of velocity potential, dynamic pressure and water elevation respectively as defined in Falnes (2002). Here, $Q(t)$ is the volume flux across the internal free surface S_I and $\hat{q}$ is the corresponding complex amplitude, positive volume flux is chosen as measured z-axis upward.

Combining (1)~~(1)~~ to (8)~~(8)~~, we have

$$\nabla^2\hat{\phi} = 0, \quad \text{in the whole fluid domain} \tag{9}$$

$$\hat{\phi}_n = 0, \quad \text{at sea bed and OWC device body surface} \tag{10}$$

$$K\hat{\phi} + \frac{\partial\hat{\phi}}{\partial z} = \begin{cases} \dfrac{-i\omega\hat{p}}{\rho g}, & \text{on } S_I \\ 0, & \text{on } S_E \end{cases} \tag{11}$$

where $K = \omega^2 / g$.

Following Evans (1982), we decompose the time-independent potential into scattering potential, $\hat{\phi}^S$, caused by an unit amplitude incident wave coming from infinity when the OWC is soild. Radiation potential, $\hat{\phi}_R$, caused by the OWC oscillating in the absence of incident wave. Both of the two potential satisfy Eq. (9)~~(9)~~ to (11)~~(11)~~. Therefore

$$\hat{\phi} = \hat{\phi}^S + \hat{\phi}_R \tag{12}$$

Recall the definition of volume flux and take Eq.(12)~~(12)~~ into consideration, we have

$$\begin{aligned}\hat{q} &= -\int_{S_I} \frac{\partial \hat{\phi}}{\partial z} dS = -\int_{S_I} \frac{\partial \hat{\phi}^S}{\partial z} dS - \int_{S_I} \frac{\partial \hat{\phi}_R}{\partial z} dS \\ &= \hat{q}^S + \hat{q}_R\end{aligned} \tag{13}$$

Where $\hat{q}^S$ and $\hat{q}_R$ is volume flux induced by scattering and radiation potential respectively defined as

$$\hat{q}^S_{,R} = -\int_{S_I} \frac{\partial \hat{\phi}^S_{,R}}{\partial z} ds \tag{14}$$

Where $\hat{q}^S_{,R}$ means $\hat{q}^S$ and $\hat{q}_R$.

Following Evans (1982), the radiation potential can be further decomposed as

$$\hat{q}_R = -(\tilde{B} - i\tilde{A})\hat{p} \tag{15}$$

Where $\tilde{A}$ and $\tilde{B}$ are real components and can be directly analogous to the added mass and radiation coefficients in rigid-body system. To simplify the problem, a new radiation potential $\hat{\phi}^R$ is defined as

$$\hat{\phi}_R = -\frac{i\omega p}{\rho g}\hat{\phi}^R \tag{16}$$

Satisfying equations (9)~~(9)~~,(10)~~(10)~~ with(11)~~(11)~~ changed to

$$K\hat{\phi}^R + \frac{\partial \hat{\phi}^R}{\partial z} = \begin{cases} 1, & \text{on } S_I \\ 0, & \text{on } S_E \end{cases} \tag{17}$$

Hence

$$\hat{q}_R = -\frac{i\omega p}{\rho g}\hat{q}^R \tag{18}$$

Substitute (18)~~(18)~~ into (15)~~(15)~~ and we can get

$$\tilde{A} = -\frac{\omega}{\rho g}\mathrm{Re}\{\hat{q}^R\} \tag{19}$$

$$\hat{B} = -\frac{\omega}{\rho g}\mathrm{Im}\{\hat{q}^R\} \tag{20}$$

The mean power absorbed per unit area of the internal surface w is the time average of pressure and the volume flux over a period. This is

$$W = \frac{1}{T}\int_0^T \mathrm{Re}\{\hat{p}e^{-i\omega t}\} \cdot \mathrm{Re}\{(\hat{q}^S + \hat{q}_R)e^{-i\omega t}\} dt \tag{21}$$

After rearranging and combine(20)~~(20)~~, we have

$$w = \frac{\left|\hat{q}^S\right|^2}{8\tilde{B}} - \frac{\tilde{B}}{2}\left|\hat{p} - \frac{\hat{q}^S}{2\tilde{B}}\right|^2 \tag{22}$$

It is well known that Wells turbine has a linear characteristic between pressure and volume flow rate

$$\hat{q} = \Lambda\hat{p} \tag{23}$$

where Λ is a real control parameter. Combine equations (13)~~(13)~~ and (15)~~(15)~~ we have

$$[\Lambda + (\tilde{B} - i\tilde{A})]\hat{p} = \hat{q}^S \tag{24}$$

Finally, by substitute (24)~~(24)~~ into (22)~~(22)~~ we get

$$w = \frac{\left|\hat{q}^S\right|^2}{8\tilde{B}}\{1 - \frac{\left|\Lambda - (\tilde{B} + i\tilde{A})\right|^2}{\left|\Lambda + (\tilde{B} - i\tilde{A})\right|^2}\} \tag{25}$$

The capture width l is defined as the proportion of extracted energy to available power per unit crest length of incident wave, P_w, as

$$l = \frac{w}{P_w} \tag{26}$$

The capture factor is defined as the capture width divided by the width of the chamber. In this work, the width of the chamber is 2b, thus capture factor is equal to $l/(2b)$.

Now the work is simplified to a hydrodynamic problem via solving the inner and external potential. By defining a proper far field radiation condition, writing the potential in cylindrical coordinate system and use Galerkin method to solve the potential, the final capture factor can be calculated. Details about how to solve this problem can be referred to Evans and Poter (1997).

Unlike Evans and ~~Poter~~Porter (1997), where they estimated the capture width l by optimised Λ which equals to $(\tilde{B}^2 + \tilde{A}^2)^{1/2}$ and presented the maximum theoretical value. Present study uses, real Λ at resonant point, which is gained from our experiment. Therefore, the analytical result is calculated under constant damping effect caused by orifice.

3. Experiment facilities and procedure

3.1. Facilities

3.1.1. Wave tank

Experiment is carried out in the largest ship-model experiment wave/towing tank in UK universities, i.e. The Kelvin Hydrodynamics Laboratory which can provide highly repeatable and controllable conditions for testing of wave and tidal energy devices at moderate scale. The tank has dimensions of 76m×4.6m×2.5m. The tank is equipped with a v~~V~~ariable-water-depth-computer-controlled four-flap absorbing wave maker generating regular or irregular waves

over 0.5m height (subject to water depth) ~~is equipped~~ and high quality variable-water-depth sloping beach with reflection coefficient typically less than 5% over frequency range of interest is used to prevent the wave reflection from the end of the tank.

3.1.2. Wave probes

OWC elevation is monitored by a ~~capacitance~~ resistance wave probe. The gauge operates by measuring the current that flows between a pair of parallel stainless wires immersed in water. Then the current is converted to an output voltage that is linearly proportional to the immersed depth through electric wire to a computer. In this way, water elevation is recorded. Calibration is carried out to obtain the linear relation between the voltage and immersion by varying the immersion of the probe in still water and records the output voltage. Once the linear relation between immersion and voltage is gain, the voltage can be transfer to corresponding immersion. Calibration result shows the maximum difference between the measured value by probe and movement of the probe is around 2% in the region interested.

~~Apart~~ In addition to~~from~~ the ~~capacitance~~ resistance wave probe, one ultrasonic liquid level sensor is ~~al~~located in front of the OWC device to measure the incident wave elevation. When measuring the wave elevation, transmitter built inside the gauge releases sonic wave. Once this sonic wave meets with the water surface it will be reflected back to the gauge. When the built in receiver detects the reflected sonic wave, a timer recoding the time interval will be trigged. By multiple sonic wave velocity transporting in air and half of the time interval, the distance between probe and water surface can be calculated. The Ultrasonic liquid level sensor does not need to contact the liquid so that there is no disturbance caused by probe like capacitance probe. However, to use this type wave probe, sufficient distance between the probe and the liquid surface should be guaranteed. Therefore, it is only used to monitor the wave elevation outside the OWC chamber. Usually, calibration is done by manufacture before it is put into market, therefore no additional calibration is needed.

3.1.3. Pressure sensor

Honeywell 163PC01D75 low differential pressure transducer is used to measure the pressure difference between the pressure inside and outside air chamber by connecting one of the ports with the orifices-plate and the other opens to atmosphere. Working range of pressure sensor is ± 622.72Pa. Electrical output is in the range of 3.5V± 2.5V with 3.5V being the atmosphere.

3.1.4. Data acquisition

Spike2 data acquisition and analysis system is used to monitor, record and analyse the experiment data.

3.1.5. OWC device and PTO system

PTO is modelled using an orifice~~s~~-plate which has 8 equally positioned small orifices. Both OWC device and orifices-plate are built using acrylic plastic. Detailed dimensions of the device and orifice~~s~~-plate is listed in Table 1~~Table 1~~. where PCD stands for pitch circle diameter.

Table 1 Geometry details of OWC device and orifice plate

OWC device	overall height	inside diameter	outside diameter	draught
	1045mm	287mm	299mm	350mm
Orifice plate	diameter	thickness		
	299mm	12.5mm		
Orifices	diameter	position		
	35mm	170mm PCD		

3.1.6. Configuration

OWC device is set in the middle of tank with capacitance wave probe fixed at OWC chamber wall. Ultrasonic liquid level sensor is installed 3.4m in front of the OWC to measure incident wave elevation as illustrated in Fig 2~~Fig 2~~.

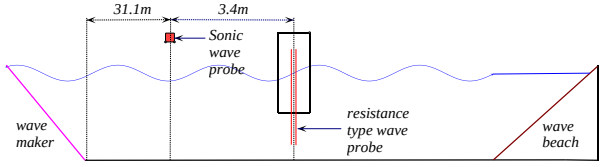

Fig 2 Configuration of the experiment

3.2. Procedures

For eliminating the temperature effect, a wall-mounted heater was switched on during the experiment to maintain the temperature at a constant of 20℃. Cases based on non-dimensionalized wave number *Kh* unequally spaced varying from 0.4 to 8.4 are investigated for zero damping (OWC open to air), low damping (4 orifices) and high damping (1 orifice). When ~~talked about~~investigating 1 and 4 orifices, the other orifices are sealed. Pressure and OWC elevation are recorded for further analysis~~e~~. ~~Designed~~ The target incident Wave amplitude is 0.03m for all testing cases. Although the sonic probe used to measure the incident wave amplitude does not touch the water, it is found that the measurement is affected by reflected and radiated wave from the OWC device. In order to get a more accurate incident wave energy estimation based on the measured wave amplitude, the wave elevation is ~~double~~ measured using the ~~capacitance~~ resistance wave probe at the location ~~where~~ of the OWC ~~device was~~, after removing the OWC device. By doing so, the difference caused by monitoring OWC and incident wave elevation with two different wave probe is minimized. However, because of time span, incident wave elevation measured without OWC device

may be slightly different from the actual incident wave. Since the wave tank can provide highly repeatable conditions, we can neglect the difference. Although great effort is made on maintaining the incident wave amplitude at the target value of 0.03m for each frequency, we still experienced minor ~~fluctuation~~ discrepancies in wave amplitude. This leads to the corresponding results slightly different from the result it should be, when incident wave amplitude is equal to 0.03m. For instance, in Fig 4~~Fig 4~~, the pressure amplitude at Kh=5.7 (as point out by arrow) is does not follow the overall trend. By referring to the measured incident wave amplitude, we noted that the measured value at Kh=5.7 is 28.322 mm, smaller than desired value. While for Kh=5.5 and 6, the measured incident wave amplitude are 29.943 mm and 29.633 mm respectively. Therefore, pressure amplitude at Kh=5.7 is lower than it should be when incident wave amplitude is equal to 0.03m.

Time derivation of OWC elevation time history gives the vertical velocity of the OWC. By assuming OWC surface is flat, we can obtain the volume flow rate simply by multiplying velocity and area of OWC surface. Based on the assumption that the phase between velocity of OWC surface and air is zero, we can calculate absorbed power according to Eq.(21)~~(21)~~ by changing it to time dependent variables. According to wave theory, the available wave power is estimated as

$$P_w = \frac{1}{2}\rho g A^2 [\frac{1}{2}\frac{\omega}{k}(1+\frac{2kh}{\sinh 2kh})] \quad (27)$$

Where A is the wave amplitude, k is wave number.

4. Results

Response amplitude operator (RAO) is a parameter used to identify the reaction level of structure under wave excitation. RAO here is defined as the response water column amplitude divided by the incoming wave amplitude. In order to validate our result against linear theory, OWC response amplitude and pressure amplitude is extracted from the original monitored data by ignoring the non-linear term. (The effect of ~~ignore~~ ignoring the non-linear effect will be ~~talked~~ discussed later)

Fig 3~~Fig 3~~ shows the RAO of OWC at 3 different conditions. It can be seen that OWC motion is more violent at lower damping. When OWC device is open to air, the Kh at which peak RAO occurs is the resonant point, namely natural frequency of OWC. (Hole in the figure means orifice and open means the OWC is open to air without any additional damping~~.~~). It is clear that two cases with orifices have shifted the resonant point more or less due to appearance of external damping.

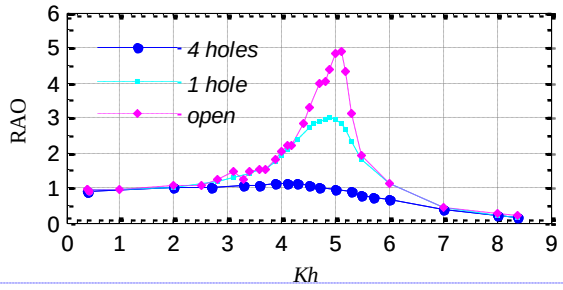

Fig 3 Response amplitude operation in frequency domain

Pressure amplitude in Fig 4~~Fig 4~~ grows with the increasing of damping on the contrary to RAO. As discussed before, the discontinuity is induced by failure to generate exactly same wave amplitude at each frequency.

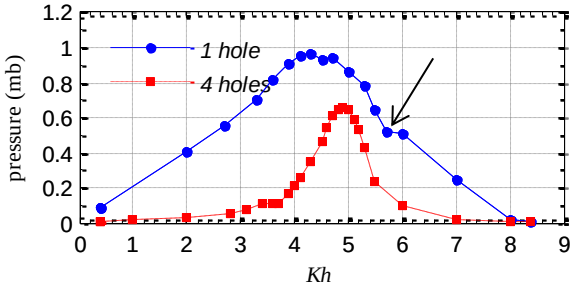

Fig 4 Pressure amplitude in frequency domain

Fig 5~~Fig 5~~, 6 and 7 show the mean captured power, capture width and capture factor respectively. For low damping case, although the peak capture factor is more than 2 times smaller than that of higher damping case, it has better performance in the range of small and large wave frequency region.

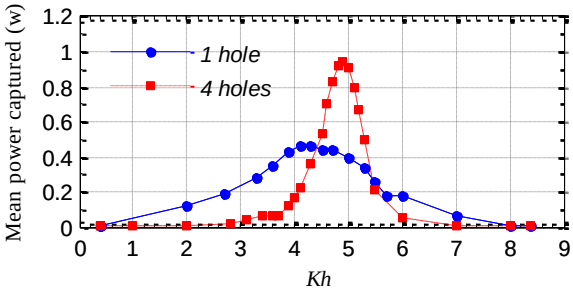

Fig 5 Mean power captured in frequency domain

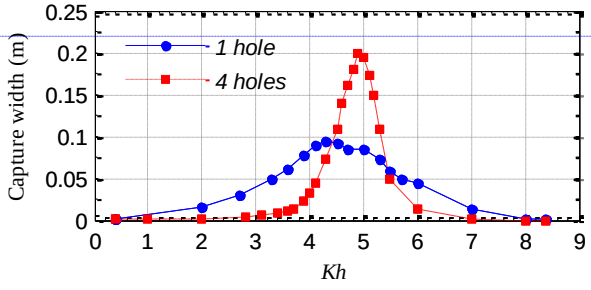

Fig 6 capture width in frequency domain

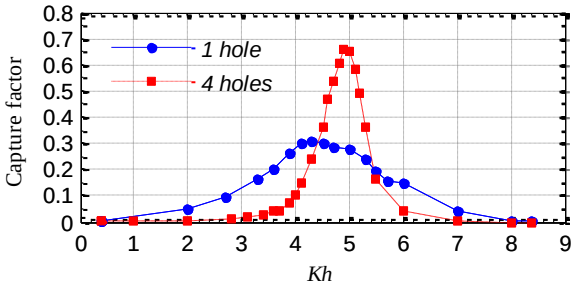

Fig 7 Capture factor in frequency domain

So far, we have neglected all non-linear terms including higher order term of wave and non-linear PTO characteristic. Since in this experiment wave is quite linear we assume the non-linear effect of wave is negligible. In the following part we will have a study on the non-linear PTO influence. Fig 8~~Fig 8~~ shows the fitted linear relation between pressure and volume flow rate and non-linear relation between them for Kh=5 with 4 orifices case. The n~~N~~on-linear relation is obtained by plotting the original time history data of one period. As we can see from Fig 8~~Fig 8~~, although the difference is apparent, the overall trend is almost identical.

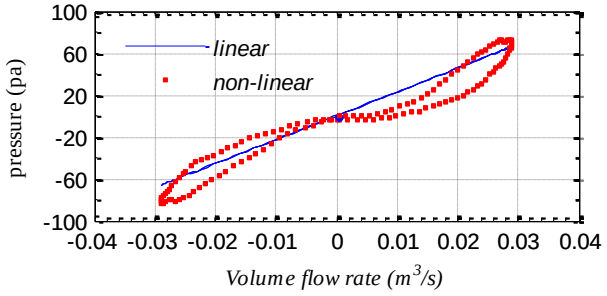

Fig 8 relation between pressure and volume flow rate

To investigate how the non-linear PTO affects the captured power, we multiply pressure with time derivation to the OWC elevation time history directly. ~~Fetch~~ Using enough periods and normalize it with time, we get the real mean power absorbed under non-linear PTO. Results are shown in Fig 9~~Fig 9~~.

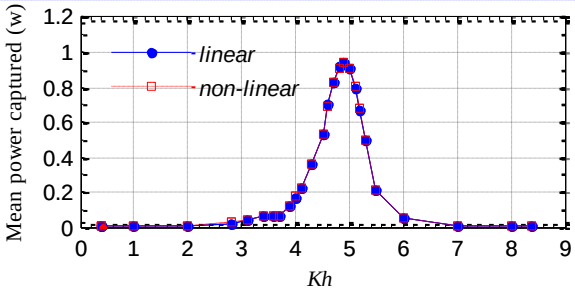

Fig 9 Comparison of mean power calculated using linear and non-linear damping

As can be seen from Fig 9~~Fig 9~~, mean power captured by two different calculation methods have negligible difference. Therefore, the capture width and capture factor are also nearly the same. This proved that it is ~~proper~~ appropriate to analyse this problem by ignoring the non-linear PTO effect.

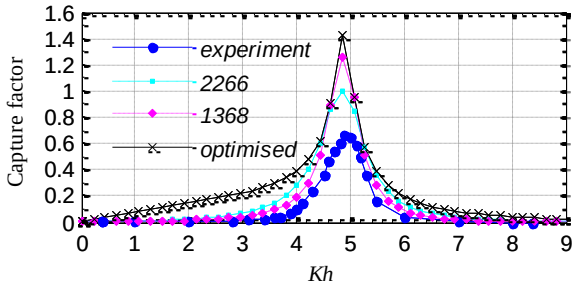

Fig 10 Comparison of experimental and analytical capture factor for 4 orifices case

Fig 10~~Fig 10~~ gives the comparison of analytical and experiment result for 4 orifices case. Where 2266 and 1368 are value of $1/\Lambda$ at Kh=5 and Kh=5.5 respectively. Since $1/\Lambda$ reflects the damping level with large number corresponding to higher damping lever, we call it damping level.

As demonstrated, under higher damping level, result matches experiment better than lower damping level around resonant point while lower damping level fits better except for resonant region. This suggests that even with the same orifice, damping effect caused by the orifice varies with OWC motion, or more strictly, the volume flow rate of the OWC.

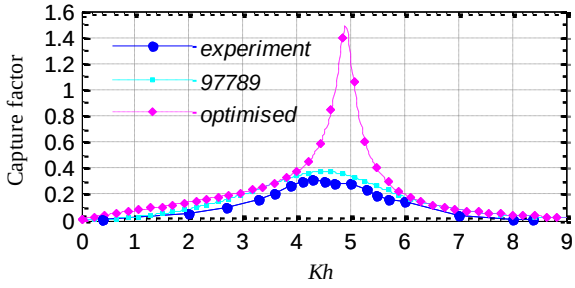

Fig 11 comparison of experimental and analytical capture factor for 1 orifice case

One orifice case has a much larger damping caused by orifice than case with 4 orifices. Analytical result is almost identical to experiment result when $1/\Lambda = 97789$ corresponding to Kh=4.1 as shown in Fig 11~~Fig 11~~. It can be seen that within lower and higher frequency region (Kh=0 to Kh=4 and Kh=6 to Kh=9), the capture factor is approximating the optimised maximum capture factor

5. Discussion and conclusion

In this work, experimental and analytical studies of a cylindrical OWC wave energy converter are carried out. Based on the result presented, following conclusion can be drawn

1. Appling an actual turbine characteristic into analytical method can provide a more reliable result than using optimised turbine characteristic.

2. Higher PTO damping leads to a better performance at low and high frequency region while low damping contributes to high capture factor around resonant region as indicated by Fig 10~~Fig 10~~.

3. Fig 11~~Fig 11~~ suggests that at high damping level, capture factor can approximate the maximum optimized value. Therefore, when design a device at field where wave frequency is relative low or high, higher damping is preferable.

One should notice that in this work, we applied the peak damping caused by orifices-plate to the analytical Eq.(25)~~(25)~~, thus it is expected that analytical result can match experiment better if we take Λ from experiment and calculate capture factor individually for each Kh. Another problem leads to difference between analytical and experimental result is the scale effect. More appropriate, the viscous effect. The difference is arisen because of that Potential theory assumes the water is ideal fluid which means the ~~Reynold's~~Reynolds number should be infinitely large, which is quite difficult to achieve in lab testing. Therefore, it is expected that when the model and wave size becomes larger, a better agreement can be achieved. On the other hand if we compare the 1 and 4 orifices cases, analytical method predict better in 1 orifices case. This is because that the motion of OWC of 1 orifice is much smaller than that of 4 orifices (Fig 3~~Fig 3~~). This leads to the energy loss of 1 orifice case due to viscous effect of OWC itself is much smaller than the energy loss in OWC of 4 orifices.

Judging by the capture width and capture factor, it seems that this kind of OWC device does have lower "efficiency" and seems not to be attractive for long-term development as proposed by Evans. However, his conclusion is drawn on the concept of wave energy device capture the power independently. If we combine the cylindrical OWC device with offshore wind turbine, the situation changed. The main structure of the device can be designed as the floater of offshore wind turbine. OWC devices can share the same power delivering system. This makes cylindrical OWC device economically attractive even though having a low "efficiency".

Acknowledgement

Strathclyde Kelvin Hydrodynamic laboratory team including ~~Mr.~~ Charles Keay, ~~Mr.~~ Grant Dunning, ~~Dr.~~ Edward Nixon, their helping in preparing, and setting up the experiment is greatly acknowledged. Visiting researcher in University of Strathclyde Dr. Islam's assisting during the experiment is also acknowledged.

Last but not the least, my colleague Mr. Zhiming Yuan's proof reading is appreciated.

Reference

Evans, D. V. (1978). The oscillating water column wave-energy device. *Journal of the Institute of Mathematics and Its Applications, 22*, 423-433.

Evans, D. V. (1982). Wave-power absorption by systems of oscillating surface pressure distributions. *Journal of Fluid Mechanics, 114*, 481-499.

Evans, D. V., & Porter, R. (1995). Hydrodynamic characteristics of an oscillating water column device. *Applied Ocean Research, 17*, 155-164.

Evans, D. V., & Poter, R. (1997). Efficienct calculation of hydrodynamcis properties of OWC-Type devices. *Journal of Off-Shore Mechanics and Arctic Engineering, 119*, 210-218.

Falcão, A. F. (2010). Wave energy utilization:A review of the technologies. *Renewable and Sustainable Energy Reviews*, 889-918.

Falnes, J. (2002). *Ocean waves and oscillating systems.* Cambridge,UK: The press syndicate of the Universtity of Cambridge.

J.J.Stoker. (1957). *Water waves.* New York: interscience publishers LTD.

Maeda, H., Kinoshita, T., Masuda, K., & Kato, W. (1985). Fundamental research on oscillating water column wave power absorbers. *Journal of Energy Resources Technology, 150*, 81-86.

Martins-Rivas, H., & Mei, C. C. (2009). Wave power extraction from an oscillating water column at the tip of a breakwater. *Journal of Fluid Mechanics, 626*, 395-414.

Mei, C. C., Stiassnie, M., & K.-P.Yue, D. (2005). *Theory and aplications of ocean surface waves.* Singapore: World Scientific Publishing Co.Pte.Ltd.

Morris-Thomas, M. T., Irvin, R. J., & Thiagarajan, K. P. (2007). An investigation into the hydrodynamic efficiency of an oscillating water column. *Journal of offshore Mechanics and Arctic Engineering, 129*, 273-278.

Newman, J. N. (1974). Interaction of water waves with two closely spaced vertical obstacles. *Journal of Fluid Mechanics, 66*, 97-106.

Sarmento, A. J. (1992). Wave flume experiments on two-dimensional oscillating water column wave energy devices. *Experiments in Fluids, 12*, 286-292.

Şentürk, U., & Özdamar, A. (2012). Wave energy extraction by an oscillating water column with a gap on the fully submerged front wall. *Applied Ocean Research, 37*, 174-182.

Thorpe, T. W. (1999). *A breif review of wave energy.* The UK Department of Trade and Industry. UK: A report produced for the UK Department of Trade and Industry.

Wang, D. J., Katory, M., & Li, Y. S. (2002). Analytical and experimental investigation on the hydrodynamic performance of onshore wave power devices. *Ocean Engineering, 29*, 871-885.

Whittaker, T. J., & Stewart, T. P. (1993). An experimental study of nearshore and shoreline oscillating water columns with harbours. *Proceedings of the European Wave Energy Symposium*, (pp. 283-288). Edinburgh,UK.